Cosmology with the thermal-kinetic Sunyaev-Zel'dovich effect

William Coulton[1],* Atsuhisa Ota[2],† and Alexander van Engelen[3,4]‡
[1] *Institute of Astronomy and Kavli Institute for Cosmology Cambridge, Madingley Road, Cambridge, CB3 0HA, UK*
[2] *Department of Applied Mathematics and Theoretical Physics, University of Cambridge, Cambridge, CB3 0WA, UK*
[3] *School of Earth and Space Exploration, Arizona State University, Tempe, AZ, 85287, USA* and
[4] *Canadian Institute for Theoretical Astrophysics, University of Toronto, 60 St George St, Toronto, ON, M5S 3H8, Canada*
(Dated: August 17, 2020)

Compton scattering of the cosmic microwave background (CMB) from hot ionized gas produces a range of effects, and the leading order effects are the kinetic and thermal Sunyaev Zel'dovich (kSZ and tSZ) effects. In the near future, CMB surveys will provide the precision to probe beyond the leading order effects. In this work we study the cosmological information content of the next order term which combines the tSZ and kSZ effects, hereafter called the thermal-kinetic Sunyaev Zel'dovich (tkSZ) effect. As the tkSZ effect has the same velocity dependence as the kSZ effect, it will also have many of the useful properties of the kSZ effect. However, it also has its own, unique spectral dependence, which allows it to be isolated from all other CMB signals. We show that with currently-envisioned CMB missions the tkSZ effect can be detected and can be used to reconstruct large scale velocity fields, with no appreciable bias from either the kSZ effect or other extragalactic foregrounds. Furthermore, since the tkSZ effect arises from the well-studied pressure of ionized gas, rather than the gas number density as in the kSZ effect, the degeneracy due to uncertain gas physics will be significantly reduced. Finally, for a very low-noise experiment the tkSZ effect will be measurable at higher precision than the kSZ effect.

Introduction—. Cosmological observations will significantly increase in size and scope in the next few decades. In particular, galaxy surveys and high resolution measurements of secondary anisotropies in the cosmic microwave background (CMB) will shed light on new aspects of cosmology [1–4]. These efforts will be powerful themselves, but taking cross-correlations of these observables will provide us further information of the Universe. One such strategy would be large scale velocity reconstruction with the kinetic Sunyaev-Zel'dovich (kSZ) effect [5], which arises from bulk flows of free electrons along the line of sight. The first detections of the kSZ effect have been obtained in the past few years, using galaxy redshift surveys together with high-resolution maps of the CMB [6–12]. The precision of these measurements will increase drastically in the near future [13–16]. These measurements are probes of both large-scale bulk flows and the smaller-scale distribution of electrons in halos. Measurements of the large-scale velocities can be used to probe primordial non-Gaussianity and the growth rate. While measurements of the latter have significant possibilities for constraining fundamental cosmology, including modifications to general relativity, it is subject to astrophysical uncertainty arising from the distribution of ionized gas within dark matter halos [16, 17]. This uncertainty is known as the "optical depth degeneracy" and several methods have been put forward to reduce it [18–20]. In this article we explore the potential of relativistic corrections to the SZ effects [21–26], which we call the thermal kinetic Sunyaev-Zel'dovich (tkSZ) effect, for velocity reconstruction. The tkSZ effect arises from the thermal pressure of electron gas in moving halos, whereas the kSZ effect arises from the gas density in moving halos; depending on the gas temperature it is about a 1% correction to the kSZ effect. It is also known as a relativistic correction to the kSZ effect [21, 24, 26], but can equally be considered a velocity correction to the tSZ effect. Its frequency dependence is different from both of the kSZ and thermal Sunyaev-Zel'dovich (tSZ) effects. Given observations with enough frequency bands, we can distinguish and isolate each of these signals. Using the recently proposed kSZ tomography technique [27], we show for the first time that the tkSZ effect is detectable via the galaxy-galaxy-tkSZ bispectrum in currently envisioned observational projects such as the Probe of Inflation and Cosmic Origins (PICO) [28] or CMB-HD experiments [29]. This work complements Ref. [30] which discussed the power spectrum of higher order thermal relativistic corrections to the tSZ effect (rtSZ hereafter); hints of the rtSZ correction, which is almost an order of magnitude larger than the tkSZ correction, have been recently seen [31, 32] and the rtSZ is one of the targets of upcoming surveys [33, 34].

Relativistic SZ effects—. The SZ effects are spectral distortions to the homogeneous and isotropic blackbody spectrum of the CMB; see Ref. [35] for a review. They are produced when the CMB photons are scattered by electrons in halos after recombination, and hence they are useful to investigate the thermodynamics of the electrons, and the peculiar motions of the halos. To compute the SZ effects, we solve the Boltzmann equations for photons including Compton scattering. For cosmology, we are interested in using the properties of many SZ sources, so we apply moment expansion schemes to simplify the calculations [23–26, 36]. Using this technique, we expand the Boltzmann equation in terms of the relativistic corrections with the single scattering approximation.

Let ν and $T_{\rm CMB} = 2.725$K be the photons' frequency and the CMB temperature today. The background phase space distribution function of the CMB is written by a Planck distribution $\bar{f} \equiv [\exp(h\nu/k_{\rm B}T_{\rm CMB}) - 1]^{-1}$, with h and $k_{\rm B}$ being the Planck and Boltzmann constants. We Taylor expand the CMB distribution function, f, around $\bar{f}$ in terms of the electron temperature-mass ratio $\theta_{\rm e} \equiv k_{\rm B}T_{\rm e}/m_{\rm e}c^2$, and the halos' 3-velocity $\boldsymbol{v}$. Defining the derivative operator $\mathcal{D} \equiv -\nu\partial/\partial\nu$, we introduce two functions of photon frequency ν: $\mathcal{G} \equiv \mathcal{D}\bar{f}$, and $\mathcal{Y} \equiv (\mathcal{D}^2 - 3\mathcal{D})\bar{f}$. $\mathcal{G}$ is the frequency dependence of the primary temperature anisotropies, and $\mathcal{Y}$ is that of the Compton y parameter. We generalize the n-th derivatives of the Planck distribution in terms of ν as $\mathcal{Y}^{(n)} \equiv \mathcal{D}^{n-2}\mathcal{Y}$ for $n \geq 2$. Using these functions, we write the spectral distortion $\delta f \equiv f - \bar{f}$ due to the Compton scattering in halos as [23–26]

$$\delta f = \int {\rm d}\chi n_{\rm e}\sigma_{\rm T} a S, \tag{1}$$

where $n_{\rm e}$, a, and χ are electron number density in the cluster rest frame, the scale factor and the comoving distance, and the source function is [24, 26, 37]

$$\begin{aligned} S = \theta_{\rm e}\mathcal{Y}^{(2)} + \theta_{\rm e}^2\left(-\frac{3}{10}\mathcal{Y}^{(2)} - \frac{21}{10}\mathcal{Y}^{(3)} + \frac{7}{10}\mathcal{Y}^{(4)}\right) \\ + \boldsymbol{v}\cdot\mathbf{n}\mathcal{G} + \theta_{\rm e}\boldsymbol{v}\cdot\mathbf{n}\left(\frac{2}{5}\mathcal{G} - \mathcal{Y}^{(2)} + \frac{7}{5}\mathcal{Y}^{(3)}\right) + \cdots, \end{aligned} \tag{2}$$

with line-of-sight direction $\mathbf{n}$. These terms correspond respectively to the tSZ, rtSZ, kSZ, and tkSZ effects, the latter of which is the focus of this paper. We have dropped higher order corrections in terms of $\theta_{\rm e}$ and $\boldsymbol{v}\cdot\mathbf{n}$ as they are subdominant for typical halos [24, 26]. We assumed that the halo's incoming photon distributions are the homogeneous and isotropic Planck distribution. Note that the optical depth in the CMB rest frame depends on the halos' velocity, and $-\mathcal{Y}^{(2)}$ in the second line is a frequency shift because of this effect [37]. Eq. (1) evaluated on the sky can be factored into its dependence on line-of-sight direction and frequency according to

$$\delta f(\nu, \mathbf{n}) = \Theta(\mathbf{n})\mathcal{G}(\nu) + y(\mathbf{n})\mathcal{Y}(\nu) + \alpha(\mathbf{n})\mathcal{A}(\nu) + \ldots, \tag{3}$$

where $\Theta(\mathbf{n})$ is a dimensionless temperature perturbation composed of the primary anisotropy, kSZ and integrated Sachs-Wolfe (ISW) effects. $\mathcal{A}(\nu) \equiv 2\mathcal{G}(\nu)/5 - \mathcal{Y}^{(2)}(\nu) + 7\mathcal{Y}^{(3)}(\nu)/5$ is the frequency response for the tkSZ effect parameterized by $\alpha(\mathbf{n})$. Combining Eqs. (1) and (3), we obtain

$$\alpha = \int {\rm d}\chi R p\frac{\boldsymbol{v}}{c}\cdot\mathbf{n}, \quad R \equiv \frac{a\sigma_{\rm T}}{m_{\rm e}c^2}, \tag{4}$$

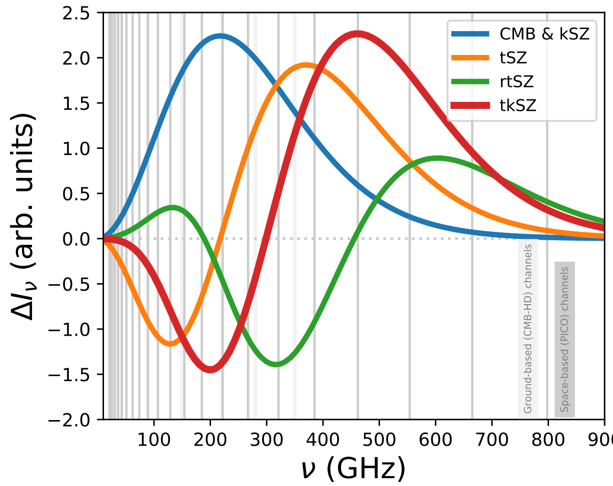

FIG. 1. Spectral response for the kSZ effect (blue, $\propto \nu^3\mathcal{G}$), the tSZ effect (orange), the tkSZ effect (red) and the rtSZ (green). The frequency bands for the experiments we consider are shown in grey.

where $p \equiv n_{\rm e}k_{\rm B}T_{\rm e}$ is the electron pressure. This effect can be contrasted with the tSZ effect $y = \int {\rm d}\chi R p$, and the kSZ effect $\Theta_{\rm kSZ} = \int {\rm d}\chi a\sigma_T n_{\rm e}\boldsymbol{v}/c\cdot\mathbf{n}$. Thus the calculation of the tkSZ effect is identical to the kSZ, effect except the electron density is replaced by the pressure.

Isolating the signal—. The sky is composed of many different signals, and to study the very faint tkSZ effect we need to isolate it from the other backgrounds. Given observations with enough frequency channels we can use the unique spectral signature in Fig. 1 to isolate the tkSZ effect from the other sky signals. We use the constrained internal linear combination (cILC) method [38] to do this and to ensure that there is no contamination from the larger kSZ effect with similar velocity dependence. Due to the tkSZ's velocity dependence, there is no bias to our detection methods (described below) from the tSZ or cosmic infrared background (CIB), but these signals contribute effective noise. The cILC approach is constructed to yield minimum-noise maps of the tkSZ effect, but with zero response to the kSZ. This is enabled by our perfect knowledge of the spectrum of both signals. We summarize this method here and refer the reader to Ref. [38] for more details. The measured intensity at a frequency ν_i, $s_i(\mathbf{n})$, can be given by discretizing Eq. (3), with the appropriate phase space volume element

$$s_i(\mathbf{n}) = \alpha(\mathbf{n})A_i + \Theta(\mathbf{n})G_i + N_i(\mathbf{n}), \tag{5}$$

where $G_i \equiv 2h\nu_i^3c^{-2}\mathcal{G}(\nu_i)$ is a vector of the spectral dependencies of the CMB, ISW and kSZ effects, and $A_i \equiv 2h\nu_i^3c^{-2}\mathcal{A}(\nu_i)$ is that of the tkSZ effect at the observed frequencies. The $N_i(\mathbf{n})$ are all other signals, which we assume consist of: tSZ, rtSZ, CIB, radio galaxies, galactic dust emission, instrumental noise and, for ground-based surveys, atmospheric noise. In Table I we summarize the spatial and spectral properties of these components. We assume that the CIB and tSZ are correlated at the 10% level [39] and the rtSZ, tSZ, tkSZ and kSZ correlations are described by the halo model. For simplicity we do not allow for frequency decoherence of the CIB. For the amplitude of the power spectrum of dust, we assume the measurement of Ref. [40], which is a fit to a relatively small fraction of sky; however, we found that our results are unchanged if the amplitude of galactic dust power is increased by a factor of ten.

We consider two reference experiments. First, a space-based survey with extensive frequency coverage. Our setup is based on the recently proposed PICO experiment [28]. The PICO satellite would have 23 frequency channels, shown as vertical bars in Fig. 1; in its most sensitive channel, 154 GHz, it has a sensitivity of 1.5 μK-arcmin and resolution of 6.2 arcmin. Secondly, a ground-based survey, with reduced frequency coverage but significantly higher angular resolution. We adopt the parameters of the recently-envisioned CMB-HD experiment [29], with 7 frequency channels and a maximal sensitivity of 0.7 μK-arcmin and resolution of 0.42 arcmin at 90 GHz. We forecast the statistics of the isolated tkSZ map by using the cILC estimator:

$$\hat{\alpha} = \frac{(\vec{G}\cdot\Sigma^{-1}\vec{G})\vec{A} - (\vec{A}\cdot\Sigma^{-1}\vec{G})\vec{G}}{(\vec{A}\cdot\Sigma^{-1}\vec{A})(\vec{G}\cdot\Sigma^{-1}\vec{G}) - (\vec{A}\cdot\Sigma^{-1}\vec{G})^2}\cdot\Sigma^{-1}\vec{s}, \quad (6)$$

where the matrix $\Sigma_{ij} = \langle s_i s_j\rangle$ is the covariance between observed signals at frequency i and j. In harmonic space, Σ is reduced to the observed cross power spectra at multipole ℓ. Using this formalism the power spectrum of the isolated tkSZ signal, $\widehat{C}_\ell^{\alpha\alpha}$, is

$$\widehat{C}_\ell^{\alpha\alpha} = \frac{\vec{G}\cdot\Sigma_\ell^{-1}\vec{G}}{(\vec{A}\cdot\Sigma_\ell^{-1}\vec{A})(\vec{G}\cdot\Sigma_\ell^{-1}\vec{G}) - (\vec{A}\cdot\Sigma_\ell^{-1}\vec{G})^2}, \quad (7)$$

which includes the signal, experimental noise and residual foregrounds. The resulting spectra, dominated by noise and residual foregrounds, are shown in Fig. 2 for our two experiments. We note that the constraint of demanding zero response to the kSZ comes at the cost of increasing the variance of the tkSZ map on small angular scales by a factor of 4 (for the ground based experiment); however, to be conservative we include this constraint in our forecasts below.

The tkSZ power spectrum—. We extend the formalism in Ref. [42] to compute the tkSZ power spectrum. This is done by replacing the electron density in the kSZ power spectrum with the electron pressure. Thus the tkSZ power spectrum is

$$C_\ell^{\alpha\alpha} = \frac{1}{2}\int\frac{\mathrm{d}\chi}{\chi^2}(RaH)^2 f^2\int\frac{\mathrm{d}^3k'}{(2\pi)^3}\Big(P_{pp}(|\mathbf{k}-\mathbf{k}'|,z) \times P_{\delta\delta}^{\mathrm{lin}}(k',z)\frac{k(k-2k'\mu')(1-\mu'^2)}{k'^2(k^2+k'^2-2kk'\mu')}\Big)\Big|_{k=\frac{\ell}{\chi}}, \quad (8)$$

TABLE I. Spectral and spatial dependence of the foregrounds we include in isolating the tkSZ effect. Here, $B_\nu(T)$ is the spectral radiance of a blackbody at the CIB or dust temperature. We use Refs. [40, 41] for the foreground parameters.

Component	Spectral dependence	Spatial dependence
CMB +kSZ	$\propto \nu^3\mathcal{G}$	$C_\ell^{\Theta\Theta}$
tSZ	$\propto \nu^3\mathcal{Y}$	C_ℓ^{yy}
CIB	$\propto \nu^{\beta_{\mathrm{CIB}}}B_\nu(T_{\mathrm{CIB}})$	$A_p^{\mathrm{CIB}} + A_c(\ell/\ell_c)^{\alpha_{\mathrm{CIB}}}$
Radio	$\propto \nu^{\beta_{\mathrm{Radio}}}$	$A_{\mathrm{Radio}}(\ell/\ell_c)^{\alpha_{\mathrm{Radio}}}$
Galactic Dust	$\propto \nu^{\beta_{\mathrm{Dust}}}B_\nu(T_{\mathrm{Dust}})$	$A_{\mathrm{Dust}}(\ell/\ell_c)^{\alpha_{\mathrm{Dust}}}$

where H is the Hubble parameter, f is the logarithmic derivative of the growth factor ($\mathrm{d}\log D/\mathrm{d}\log a$), $\mu' = \hat{\mathbf{k}}\cdot\hat{\mathbf{k}}'$ and $P_{\delta\delta}^{\mathrm{lin}}$ is linear matter power spectrum. We use the halo model [43] to compute the non-linear pressure power spectrum P_{pp}, using a modified version of the hmvec code [44] and with the cluster pressure profiles from Ref. [45]. In addition we compute the cross power spectrum with the kSZ effect, using the electron density profiles from Ref. [46].

One may wonder if we are able to directly observe the tkSZ power spectrum or tkSZ-kSZ cross power spectrum by exploiting the specific frequency dependence of the tkSZ effect. However, we find that measuring these correlations is difficult as the auto-spectrum is tiny and, at large scales, the cross spectrum is limited by the CMB noise from the primary CMB (which cannot be separated from the kSZ). These power spectra are shown in Fig. 2. We see that the signal is beyond the detection capabilities of upcoming experiments.

The galaxy-galaxy-tkSZ bispectrum—. Several methods have been used for detecting the kSZ effect from galaxy survey. These include stacking differences of the CMB temperature at locations of objects [6, 7, 47, 48], as well as performing a velocity-weighted stack of CMB temperatures on the objects, in which the velocities are obtained from a three-dimensional map of structure [11, 12]. Ref. [27] showed that these methods are all measures of the galaxy-galaxy-kSZ bispectrum, which is a sensitive probe of cosmological parameters [16, 49]. The velocity dependence of the tkSZ effect means that we can utilise the same machinery to study the galaxy-galaxy-tkSZ bispectrum, which is the main result of this paper. Following Ref. [27], we use a simplified 'snapshot' geometry to approximate cross correlations with galaxy surveys. This geometry simplifies the light cone evolution effects. We model the universe as a periodic 3D box with comoving side length L at a snapshotted redshift z_* and use $*$ to denote quantities at this snapshotted time. We also work in the flat-sky approximation, assuming the sky to be periodic with angular side length L/χ_*.

We decompose the observed galaxy density field, $g(\mathbf{x})$ and tkSZ map, $\alpha(\boldsymbol{n})$, into Fourier compo-

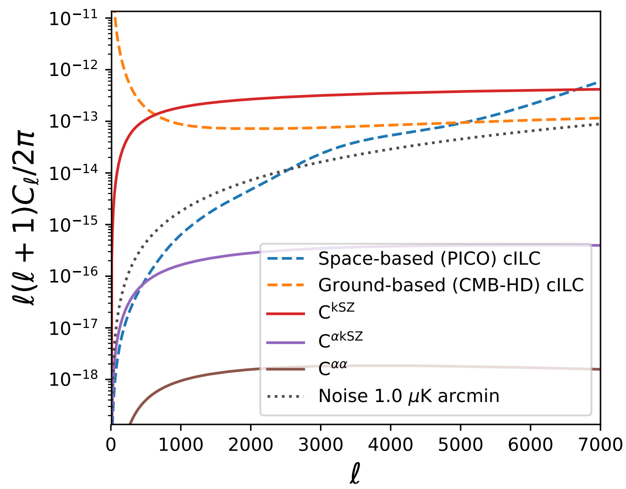

FIG. 2. The tkSZ auto spectrum (brown) and its cross correlation with the kSZ effect (purple). Also plotted are the constrained ILC noise curves for the CMB-HD (dashed orange) and PICO-like experiments (dashed blue). For scale, we plot the kSZ power spectrum (red) and the 1 μK-arcmin noise curve (dotted).

nents as $g(\mathbf{k}) \equiv \int \mathrm{d}^3\mathbf{x} g(\mathbf{x}) e^{-i\mathbf{k}\cdot\mathbf{x}}$, and $\alpha(\boldsymbol{\ell}) \equiv \int \mathrm{d}^2\boldsymbol{n}\alpha(\boldsymbol{n})e^{-i\boldsymbol{n}\cdot\boldsymbol{\ell}}$. Symmetries simplify the momentum dependence of the bispectrum and we find $\langle g(\mathbf{k})g(\mathbf{k}')\alpha(\boldsymbol{\ell})\rangle' = iB_{gg\alpha}(k, k', \ell, k_r)$ [27], where the prime on the bracket implies that we omitted $(2\pi)^3\delta^{(3)}\left(\mathbf{k}+\mathbf{k}'+\boldsymbol{\ell}/\chi_*\right)$. Ref. [27] showed that the signal to noise ratio (SNR) is dominated by squeezed configurations, i.e. $k_L \ll k_S \sim \ell/\chi_*$ and we confirm that this is also the case for the tkSZ. With the approximations of Ref. [27], that the squeezed bispectrum can be approximated by the tree level bispectrum with the linear power spectra replaced by the non linear power spectra, we find

$$B_{gg\alpha} \approx \frac{R_* k_r}{\chi_*^2}\left[\frac{P_{gv}(k')}{k'}P_{gp}(k) - \frac{P_{gv}(k)}{k}P_{gp}(k')\right], \quad (9)$$

where $P_{XY} \equiv \langle X(\mathbf{k})Y(\mathbf{k}')\rangle'$ are the cross power spectra of X and Y. To compute the non-linear $P_{gp}(k)$ we use the halo model [43], the galaxy HOD [50, 51] from Refs. [52, 53] and the cluster pressure profiles from Ref. [45]. With these approximations, the SNR is given by

$$\mathrm{SNR}^2 = \frac{VR_*^2}{12\pi^3\chi_*^2}\int \mathrm{d}q_L \mathrm{d}q_S \frac{q_L^2 P_{gv}^2(q_L)}{P_{gg}^{\mathrm{tot}}(q_L)}\frac{q_S P_{gp}^2(q_S)}{P_{gg}^{\mathrm{tot}}(q_S)\widehat{C}^{\alpha\alpha}_{k_S\chi_*}}. \quad (10)$$

Note that the derivation of Eq. (10) is parallel to that of kSZ tomography in [27] with the replacement of n_e with p. We consider how our two reference experiments can be combined with an upcoming DESI-like spectroscopic survey [4] to measure the tkSZ bispectrum. We assume the mean redshift of the galaxy survey is 0.75, that the volume of overlap with the CMB survey is 116 Gpc^3, the galaxy bias is 1.51 and the observed galaxy number density 1.7×10^{-4} Mpc^{-3}.

We find that both experiments would be able to detect the galaxy-galaxy-tkSZ bispectrum at the $\sim 8\sigma$ level. Note that the experiments achieve this SNR from different scales, with CMB-HD gaining information from much smaller scales. In Fig. 3 we explore the detectability as the experimental noise level in all channels is scaled by the same factor, finding that a 3σ detection would still be possible from either survey if the map-level noise were increased by a factor of ~ 4 A key requirement to detect this signal is a wide range of frequencies with low noise, in order to separate the foregrounds and deproject the kSZ signal. For an upcoming ground-based survey with more modest angular resolution than CMB-HD, namely CMB-S4 [54] used together with CCAT-prime for the higher frequencies [55], we find a marginal detection prospect of 2.1σ. Additionally we note that, as our constraints are limited by the noise in the CMB leg, other spectroscopic surveys will only be able to detect this signal at a similar significance. For example a Euclid like survey, based on the configuration in [56], in combination with either CMB-HD or PICO, would have a detection significance of $\sim 6\sigma$. Note that in the longer term, this effect could be detected at a very high significance: we find that the cosmic variance limit SNR (with an $\ell_{\max} = 5000$) is 1340, assuming the covariance matrix only has Gaussian contributions. This is higher than the equivalent CV limit for the kSZ effect, as the kSZ SNR is limited by the primary CMB and reionization kSZ signals that act as noise.

In this work the only systematic uncertainty we have accounted for is the impact of other signals in the CMB maps as this is expected to be the main potential systematic. The parity odd nature of the signal, as well as the largely independent systematics in the galaxy and CMB components, means this should be a robust measurement. One other potential systematic is redshift space uncertainties; Ref. [27] explored how these would impact such bispectrum analyses. For a photometric survey this effect can strongly degrade the constraints, but spectroscopic surveys (such as DESI and Euclid as considered here) are unaffected. Finally we investigated how uncertainties in the gas pressure distribution affect our results. We found that 10% variations in the amplitude of the pressure cluster-mass relation and the spectral index of the pressure profile resulted in $< 10\%$ changes in the SNR ratio. Finally, a simple investigation of the impact of CIB decoherence found that the results from the ground based experiment are robust to CIB decoherence, however the space based mission could be degraded by up to a factor of a two.

Conclusion—. In this work we have identified tkSZ effect as a new cosmological observable. As a higher-order SZ effect it is a small signal, however we have found that this signal would be detectable by the envisioned PICO

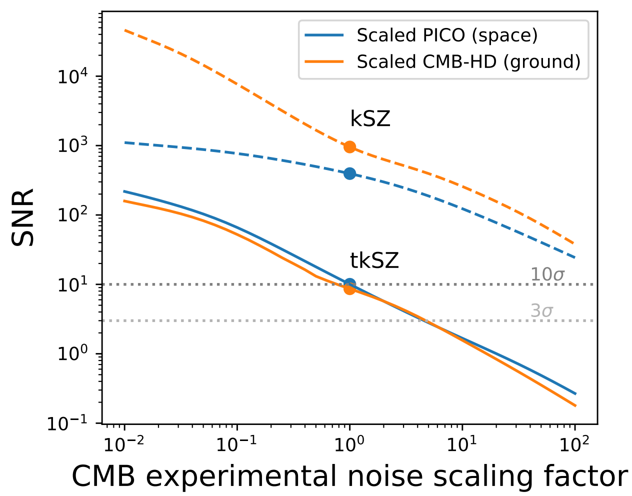

FIG. 3. Signal to noise ratio for the galaxy-galaxy-tkSZ as would be obtained using methods similar to current methods to constrain the kSZ effect, with our baseline experiments showing $\sim 8\sigma$ forecasts (circles). On the horizontal axis we scale these nominal map level instrumental sensitivities at all frequencies by the amount shown, in order to demonstrate the impact on the SNR. For context, we plot, with dashed lines, the equivalent SNR for the galaxy-galaxy-kSZ signal.

and CMB-HD experiments when combined with DESI or Euclid. This is achievable due two features of the signal: firstly, as the signal has a unique spectral signature; and secondly, the velocity dependence of the signal means that it has a vanishing cross-correlation with most other sky signals.

Whilst we have focused on outlining the origin and detectability of this effect, there are several interesting potential applications. Perhaps most interestingly, we can use the galaxy-galaxy-tkSZ bispectrum to reconstruct the large scale velocity field. This can used to constrain primordial non-Gaussianity and modifications to GR [16, 17, 57].

For the later goal, tkSZ tomography would be highly complementary to standard kSZ tomography; primarily as the tkSZ approach could aid the optical depth problem. This arises for kSZ tomography as the distribution of electrons is uncertain and means that velocity reconstruction methods have an unknown normalization. This is not the case for the tkSZ, since it instead depends on the cluster pressure profile, which can be determined by tSZ measurements to a much higher precision than the electron distribution. Finally, we note that in the longer term, the tkSZ power spectrum could be measured, instead of the cross bispectrum discussed here. tkSZ power spectrum measurements would directly probe the large scale pressure-velocity power spectrum, though we defer a thorough discussion of this to the future.

We would like to thank Anthony Challinor, Jens Chluba, Colin Hill, Neelima Sehgal, and Kendrick Smith for helpful discussions. AO is suppoted by Japan Society of Promotion of Science Overseas Research Fellowships. AvE would like to thank the Kavli Institute for Cosmology Cambridge for their support and hospitality for his visit under their Visiting Scholars program, during which this work was initiated. The “hmvec” halo model code made by Mathew Madhavacheril was used in this analysis. WRC acknowledges support from the UK Science and Technology Facilities Council (grant number ST/N000927/1).

---

* wcoulton@ast.cam.ac.uk
† a.ota@damtp.cam.ac.uk
‡ alexander.van.engelen@asu.edu

[1] James Aguirre et al. The Simons Observatory: Science Goals and Forecasts. JCAP, 1902:056, 2019. arXiv:1808.07445, doi:10.1088/1475-7516/2019/02/056.

[2] Kevork N. Abazajian et al. Cmb-S4 Science Book, First Edition. 2016. arXiv:1610.02743.

[3] Paul A. Abell et al. Lsst Science Book, Version 2.0. 2009. arXiv:0912.0201.

[4] Amir Aghamousa et al. The Desi Experiment Part I: Science,Targeting, and Survey Design. 2016. arXiv:1611.00036.

[5] R. A. Sunyaev and Ya. B. Zeldovich. The Velocity of clusters of galaxies relative to the microwave background. The Possibility of its measurement. Mon. Not. Roy. Astron. Soc., 190:413–420, 1980.

[6] Nick Hand et al. Evidence of Galaxy Cluster Motions with the Kinematic Sunyaev-Zel'dovich Effect. Phys. Rev. Lett., 109:041101, 2012. arXiv:1203.4219, doi:10.1103/PhysRevLett.109.041101.

[7] F. De Bernardis et al. Detection of the Pairwise Kinematic Sunyaev-Zel'dovich Effect with Boss Dr11 and the Atacama Cosmology Telescope. JCAP, 1703(03):008, 2017. arXiv:1607.02139, doi:10.1088/1475-7516/2017/03/008.

[8] B. Soergel et al. Detection of the kinematic Sunyaev–Zel'dovich effect with DES Year 1 and SPT. Mon. Not. Roy. Astron. Soc., 461(3):3172–3193, 2016. arXiv:1603.03904, doi:10.1093/mnras/stw1455.

[9] J. Colin Hill, Simone Ferraro, Nick Battaglia, Jia Liu, and David N. Spergel. Kinematic Sunyaev-Zel'dovich Effect with Projected Fields: A Novel Probe of the Baryon Distribution with Planck, WMAP, and WISE Data. Phys. Rev. Lett., 117(5):051301, 2016. arXiv:1603.01608, doi:10.1103/PhysRevLett.117.051301.

[10] N. Aghanim et al. Planck Intermediate Results. Liii. Detection of Velocity Dispersion from the Kinetic Sunyaev-Zeldovich Effect. Astron. Astrophys., 617:A48, 2018. arXiv:1707.00132, doi:10.1051/0004-6361/201731489.

[11] Emmanuel Schaan, Simone Ferraro, Mariana Vargas-Magaña, Kendrick M. Smith, Shirley Ho, Simone Aiola, Nicholas Battaglia, J. Richard Bond, Francesco De Bernardis, Erminia Calabrese, Hsiao-Mei Cho, Mark J. Devlin, Joanna Dunkley, Patricio A. Gallardo, Matthew Hasselfield, Shawn Henderson, J. Colin Hill, Adam D. Hincks, Renée Hlozek, Johannes Hub-

mayr, John P. Hughes, Kent D. Irwin, Brian Koopman, Arthur Kosowsky, Dale Li, Thibaut Louis, Marius Lungu, Mathew Madhavacheril, Loïc Maurin, Jeffrey John McMahon, Kavilan Moodley, Sigurd Naess, Federico Nati, Laura Newburgh, Michael D. Niemack, Lyman A. Page, Christine G. Pappas, Bruce Partridge, Benjamin L. Schmitt, Neelima Sehgal, Blake D. Sherwin, Jonathan L. Sievers, David N. Spergel, Suzanne T. Staggs, Alexander van Engelen, Edward J. Wollack, and ACTPol Collaboration. Evidence for the kinematic Sunyaev-Zel'dovich effect with the Atacama Cosmology Telescope and velocity reconstruction from the Baryon Oscillation Spectroscopic Survey. Phys. Rev. D, 93(8):082002, Apr 2016. arXiv:1510.06442, doi:10.1103/PhysRevD.93.082002.

[12] Yin-Zhe Ma, Guo-Dong Gong, Ning Sui, and Ping He. Constraining the optical depth of galaxies and velocity bias with cross-correlation between the kinetic Sunyaev–Zeldovich effect and the peculiar velocity field. Mon. Not. Roy. Astron. Soc., 475(1):379–390, 2018. arXiv:1711.08756, doi:10.1093/mnras/stx3063.

[13] Moritz Münchmeyer, Mathew S. Madhavacheril, Simone Ferraro, Matthew C. Johnson, and Kendrick M. Smith. Constraining local non-Gaussianities with kSZ tomography. 2018. arXiv:1810.13424.

[14] Simone Ferraro, J. Colin Hill, Nick Battaglia, Jia Liu, and David N. Spergel. Kinematic Sunyaev-Zel'dovich effect with projected fields. II. Prospects, challenges, and comparison with simulations. Phys. Rev., D94(12):123526, 2016. arXiv:1605.02722, doi:10.1103/PhysRevD.94.123526.

[15] Anne-Sylvie Deutsch, Emanuela Dimastrogiovanni, Matthew C. Johnson, Moritz Münchmeyer, and Alexandra Terrana. Reconstruction of the remote dipole and quadrupole fields from the kinetic Sunyaev Zel'dovich and polarized Sunyaev Zel'dovich effects. Phys. Rev., D98(12):123501, 2018. arXiv:1707.08129, doi:10.1103/PhysRevD.98.123501.

[16] Zhen Pan and Matthew C. Johnson. Forecasted Constraints on Modified Gravity from Sunyaev Zel'dovich Tomography. 2019. arXiv:1906.04208.

[17] David Alonso, Thibaut Louis, Philip Bull, and Pedro G. Ferreira. Reconstructing cosmic growth with kinetic Sunyaev-Zel'dovich observations in the era of stage IV experiments. Phys. Rev., D94(4):043522, 2016. arXiv:1604.01382, doi:10.1103/PhysRevD.94.043522.

[18] Samuel Flender, Daisuke Nagai, and Michael McDonald. Constraints on the Optical Depth of Galaxy Groups and Clusters. Astrophys. J., 837(2):124, 2017. arXiv:1610.08029, doi:10.3847/1538-4357/aa60bf.

[19] Nicholas Battaglia. The Tau of Galaxy Clusters. JCAP, 1608(08):058, 2016. arXiv:1607.02442, doi:10.1088/1475-7516/2016/08/058.

[20] Mathew S. Madhavacheril, Nicholas Battaglia, Kendrick M. Smith, and Jonathan L. Sievers. Cosmology with Ksz: Breaking the Optical Depth Degeneracy with Fast Radio Bursts. 2019. arXiv:1901.02418.

[21] S. Y. Sazonov and R. A. Sunyaev. Cosmic Microwave Background Radiation in the Direction of a Moving Cluster of Galaxies with Hot Gas: Relativistic Corrections. ApJ, 508(1):1–5, Nov 1998. doi:10.1086/306406.

[22] S. Y. Sazonov and R. A. Sunyaev. Spectral distortions of the cosmic microwave background radiation due to interaction with the hot gas in a moving cluster: Inclusion of relativistic effects. Astronomy Letters, 24:553–567, September 1998.

[23] A. D. Challinor and A. N. Lasenby. Relativistic Corrections to the Sunyaev-Zel'dovich Effect. Astrophys. J., 499:1, 1998. arXiv:astro-ph/9711161, doi:10.1086/305623.

[24] Anthony Challinor and Anthony Lasenby. Comptonization of an Isotropic Distribution in Moving Media: Higher-Order Effects. Astrophys. J., 510:930, 1999. arXiv:astro-ph/9805329, doi:10.1086/306627.

[25] Naoki Itoh, Yasuharu Kohyama, and Satoshi Nozawa. Relativistic Corrections to the Sunyaev-Zel'dovich Effect for Clusters of Galaxies. Astrophys. J., 502:7–15, 1998. arXiv:astro-ph/9712289, doi:10.1086/305876.

[26] Satoshi Nozawa, Naoki Itoh, and Yasuharu Kohyama. Relativistic Corrections to the Sunyaev-Zel'dovich Effect for Clusters of Galaxies. 2. Inclusion of Peculiar Velocities. Astrophys. J., 508:17–24, 1998. arXiv:astro-ph/9804051, doi:10.1086/306401.

[27] Kendrick M. Smith, Mathew S. Madhavacheril, Moritz Münchmeyer, Simone Ferraro, Utkarsh Giri, and Matthew C. Johnson. KSZ tomography and the bispectrum. 2018. arXiv:1810.13423.

[28] Shaul Hanany, Marcelo Alvarez, Emmanuel Artis, Peter Ashton, Jonathan Aumont, Ragnhild Aurlien, Ranajoy Banerji, R. Belen Barreiro, James G. Bartlett, Soumen Basak, Nick Battaglia, Jamie Bock, Kimberly K. Boddy, Matteo Bonato, Julian Borrill, François Bouchet, François Boulanger, Blakesley Burkhart, Jens Chluba, David Chuss, Susan E. Clark, Joelle Cooperrider, Brendan P. Crill, Gianfranco De Zotti, Jacques Delabrouille, Eleonora Di Valentino, Joy Didier, Olivier Doré, Hans K. Eriksen, Josquin Errard, Tom Essinger-Hileman, Stephen Feeney, Jeffrey Filippini, Laura Fissel, Raphael Flauger, Unni Fuskeland, Vera Gluscevic, Krzysztof M. Gorski, Dan Green, Brandon Hensley, Diego Herranz, J. Colin Hill, Eric Hivon, Renée Hložek, Johannes Hubmayr, Bradley R. Johnson, William Jones, Terry Jones, Lloyd Knox, Al Kogut, Marcos López-Caniego, Charles Lawrence, Alex Lazarian, Zack Li, Mathew Madhavacheril, Jean-Baptiste Melin, Joel Meyers, Calum Murray, Mattia Negrello, Giles Novak, Roger O'Brient, Christopher Paine, Tim Pearson, Levon Pogosian, Clem Pryke, Giuseppe Puglisi, Mathieu Remazeilles, Graca Rocha, Marcel Schmittfull, Douglas Scott, Peter Shirron, Ian Stephens, Brian Sutin, Maurizio Tomasi, Amy Trangsrud, Alexander van Engelen, Flavien Vansyngel, Ingunn K. Wehus, Qi Wen, Siyao Xu, Karl Young, and Andrea Zonca. PICO: Probe of Inflation and Cosmic Origins. arXiv e-prints, page arXiv:1902.10541, Feb 2019. arXiv:1902.10541.

[29] Neelima Sehgal, Simone Aiola, Yashar Akrami, Kaustuv Basu, Michael Boylan-Kolchin, Sean Bryan, Sebastien Clesse, Francis-Yan Cyr-Racine, Luca Di Mascolo, Simon Dicker, Thomas Essinger-Hileman, Simone Ferraro, George M. Fuller, Dongwon Han, Mathew Hasselfield, Gil Holder, Bhuvnesh Jain, Bradley Johnson, Matthew Johnson, Pamela Klaassen, Mathew Madhavacheril, Philip Mauskopf, Daan Meerburg, Joel Meyers, Tony Mroczkowski, Moritz Munchmeyer, Sigurd Naess, Daisuke Nagai, Toshiya Namikawa, Laura Newburgh, Ho Nam Nguyen, Michael Niemack, Benjamin D. Oppenheimer, Elena Pierpaoli, Emmanuel Schaan, Anze Slosar, David Spergel, Eric Switzer, Alexander van En-

gelen, and Edward Wollack. CMB-HD: An Ultra-Deep, High-Resolution Millimeter-Wave Survey Over Half the Sky. arXiv e-prints, page arXiv:1906.10134, Jun 2019. arXiv:1906.10134.

[30] Mathieu Remazeilles and Jens Chluba. Mapping the relativistic electron gas temperature across the sky. arXiv e-prints, page arXiv:1907.00916, Jul 2019. arXiv:1907.00916.

[31] Jens Erler, Kaustuv Basu, Jens Chluba, and Frank Bertoldi. Planck's view on the spectrum of the Sunyaev–Zeldovich effect. Mon. Not. Roy. Astron. Soc., 476(3):3360–3381, 2018. arXiv:1709.01187, doi:10.1093/mnras/sty327.

[32] G. Hurier. High significance detection of the tSZ effect relativistic corrections. Astron. Astrophys., 596:A61, 2016. arXiv:1701.09020, doi:10.1051/0004-6361/201629726.

[33] Avirukt Mittal, Francesco de Bernardis, and Michael D. Niemack. Optimizing measurements of cluster velocities and temperatures for CCAT-prime and future surveys. JCAP, 1802(02):032, 2018. arXiv:1708.06365, doi:10.1088/1475-7516/2018/02/032.

[34] G. J. Stacey et al. CCAT-prime: Science with an Ultra-widefield Submillimeter Observatory at Cerro Chajnantor. 2018. arXiv:1807.04354.

[35] Tony Mroczkowski et al. Astrophysics with the Spatially and Spectrally Resolved Sunyaev-Zeldovich Effects. Space Sci. Rev., 215(1):17, 2019. arXiv:1811.02310, doi:10.1007/s11214-019-0581-2.

[36] Jens CHLuba, Eric R. Switzer, Daisuke Nagai, and Kaylea Nelson. Sunyaev-Zeldovich Signal Processing and Temperature-Velocity Moment Method for Individual Clusters. Mon. Not. Roy. Astron. Soc., 430:3054, 2013. arXiv:1211.3206, doi:10.1093/mnras/stt110.

[37] Jens Chluba, Daisuke Nagai, Sergey Sazonov, and Kaylea Nelson. A Fast and Accurate Method for Computing the Sunyaev-Zeldovich Signal of Hot Galaxy Clusters. Mon. Not. Roy. Astron. Soc., 426:510, 2012. arXiv:1205.5778, doi:10.1111/j.1365-2966.2012.21741.x.

[38] Mathieu Remazeilles, Jacques Delabrouille, and Jean-François Cardoso. CMB and SZ effect separation with constrained Internal Linear Combinations. MNRAS, 410(4):2481–2487, Feb 2011. arXiv:1006.5599, doi:10.1111/j.1365-2966.2010.17624.x.

[39] P. A. R. Ade et al. Planck 2015 results. XXIII. The thermal Sunyaev-Zeldovich effect–cosmic infrared background correlation. Astron. Astrophys., 594:A23, 2016. arXiv:1509.06555, doi:10.1051/0004-6361/201527418.

[40] J. Dunkley, E. Calabrese, J. Sievers, G. E. Addison, N. Battaglia, E. S. Battistelli, J. R. Bond, S. Das, M. J. Devlin, R. Dünner, J. W. Fowler, M. Gralla, A. Hajian, M. Halpern, M. Hasselfield, A. D. Hincks, R. Hlozek, J. P. Hughes, K. D. Irwin, A. Kosowsky, T. Louis, T. A. Marriage, D. Marsden, F. Menanteau, K. Moodley, M. Niemack, M. R. Nolta, L. A. Page, B. Partridge, N. Sehgal, D. N. Spergel, S. T. Staggs, E. R. Switzer, H. Trac, and E. Wollack. The Atacama Cosmology Telescope: likelihood for small-scale CMB data. JCAP, 2013(7):025, Jul 2013. arXiv:1301.0776, doi:10.1088/1475-7516/2013/07/025.

[41] Planck Collaboration. Planck 2015 results. X. Diffuse component separation: Foreground maps. A&A, 594:A10, Sep 2016. arXiv:1502.01588, doi:10.1051/0004-6361/201525967.

[42] Chung-Pei Ma and J. N. Fry. Nonlinear Kinetic Sunyaev-Zeldovich Effect. Phys. Rev. Lett., 88(21):211301, May 2002. arXiv:astro-ph/0106342, doi:10.1103/PhysRevLett.88.211301.

[43] Asantha Cooray and Ravi Sheth. Halo models of large scale structure. Phys. Rep., 372(1):1–129, Dec 2002. arXiv:astro-ph/0206508, doi:10.1016/S0370-1573(02)00276-4.

[44] hmvec is available at https://github.com/msyriac/hmvec.

[45] N. Battaglia, J.R. Bond, C. Pfrommer, and J.L. Sievers. On the Cluster Physics of Sunyaev-Zel'dovich and X-Ray Surveys. II. Deconstructing the Thermal SZ Power Spectrum. ApJ, 758(2):75, Oct 2012. arXiv:1109.3711, doi:10.1088/0004-637X/758/2/75.

[46] N. Battaglia. The tau of galaxy clusters. JCAP, 2016(8):058, Aug 2016. arXiv:1607.02442, doi:10.1088/1475-7516/2016/08/058.

[47] Yi-Chao Li, Yin-Zhe Ma, Mathieu Remazeilles, and Kavilan Moodley. Measurement of the pairwise kinematic Sunyaev-Zeldovich effect with Planck and BOSS data. Phys. Rev. D, 97(2):023514, Jan 2018. arXiv:1710.10876, doi:10.1103/PhysRevD.97.023514.

[48] P. A. R. Ade et al. Planck intermediate results. XXXVII. Evidence of unbound gas from the kinetic Sunyaev-Zeldovich effect. Astron. Astrophys., 586:A140, 2016. arXiv:1504.03339, doi:10.1051/0004-6361/201526328.

[49] Moritz Münchmeyer, Mathew S. Madhavacheril, Simone Ferraro, Matthew C. Johnson, and Kendrick M. Smith. Constraining local non-Gaussianities with kSZ tomography. arXiv e-prints, page arXiv:1810.13424, Oct 2018. arXiv:1810.13424.

[50] Zheng Zheng, Andreas A. Berlind, David H. Weinberg, Andrew J. Benson, Carlton M. Baugh, Shaun Cole, Romeel Davé, Carlos S. Frenk, Neal Katz, and Cedric G. Lacey. Theoretical Models of the Halo Occupation Distribution: Separating Central and Satellite Galaxies. ApJ, 633(2):791–809, Nov 2005. arXiv:astro-ph/0408564, doi:10.1086/466510.

[51] Andreas A. Berlind and David H. Weinberg. The Halo Occupation Distribution: Toward an Empirical Determination of the Relation between Galaxies and Mass. ApJ, 575(2):587–616, Aug 2002. arXiv:astro-ph/0109001, doi:10.1086/341469.

[52] Alexie Leauthaud, Jeremy Tinker, Peter S. Behroozi, Michael T. Busha, and Risa H. Wechsler. A Theoretical Framework for Combining Techniques that Probe the Link Between Galaxies and Dark Matter. ApJ, 738(1):45, Sep 2011. arXiv:1103.2077, doi:10.1088/0004-637X/738/1/45.

[53] Alexie Leauthaud, Jeremy Tinker, Kevin Bundy, Peter S. Behroozi, Richard Massey, Jason Rhodes, Matthew R. George, Jean-Paul Kneib, Andrew Benson, Risa H. Wechsler, Michael T. Busha, Peter Capak, Marina Cortês, Olivier Ilbert, Anton M. Koekemoer, Oliver Le Fèvre, Simon Lilly, Henry J. McCracken, Mara Salvato, Tim Schrabback, Nick Scoville, Tristan Smith, and James E. Taylor. New Constraints on the Evolution of the Stellar-to-dark Matter Connection: A Combined Analysis of Galaxy-Galaxy Lensing, Clustering, and Stellar Mass Functions from z = 0.2 to z =1. ApJ, 744(2):159, Jan 2012. arXiv:1104.0928, doi:10.1088/0004-637X/

744/2/159.

[54] CMB-S4 parameters from https://cmb-s4.org/wiki/index.php/Survey_Performance_Expectations.

[55] Steve K. Choi, Jason Austermann, Kaustuv Basu, Nicholas Battaglia, Frank Bertoldi, Dongwoo T. Chung, Nicholas F. Cothard, Shannon Duff, Cody J. Duell, Patricio A. Gallardo, Jiansong Gao, Terry Herter, Johannes Hubmayr, Michael D. Niemack, Thomas Nikola, Dominik Riechers, Kayla Rossi, Gordon J. Stacey, Jason R. Stevens, Eve M. Vavagiakis, and Michael Vissers. Sensitivity of the Prime-Cam Instrument on the CCAT-prime Telescope. arXiv e-prints, page arXiv:1908.10451, Aug 2019. arXiv:1908.10451.

[56] Luca Amendola, Stephen Appleby, Anastasios Avgoustidis, David Bacon, Tessa Baker, Marco Baldi, Nicola Bartolo, Alain Blanchard, Camille Bonvin, Stefano Borgani, Enzo Branchini, Clare Burrage, Stefano Camera, Carmelita Carbone, Luciano Casarini, Mark Cropper, Claudia de Rham, Jörg P. Dietrich, Cinzia Di Porto, Ruth Durrer, Anne Ealet, Pedro G. Ferreira, Fabio Finelli, Juan García-Bellido, Tommaso Giannantonio, Luigi Guzzo, Alan Heavens, Lavinia Heisenberg, Catherine Heymans, Henk Hoekstra, Lukas Hollenstein, Rory Holmes, Zhiqi Hwang, Knud Jahnke, Thomas D. Kitching, Tomi Koivisto, Martin Kunz, Giuseppe La Vacca, Eric Linder, Marisa March, Valerio Marra, Carlos Martins, Elisabetta Majerotto, Dida Markovic, David Marsh, Federico Marulli, Richard Massey, Yannick Mellier, Francesco Montanari, David F. Mota, Nelson J. Nunes, Will Percival, Valeria Pettorino, Cristiano Porciani, Claudia Quercellini, Justin Read, Massimiliano Rinaldi, Domenico Sapone, Ignacy Sawicki, Roberto Scaramella, Constantinos Skordis, Fergus Simpson, Andy Taylor, Shaun Thomas, Roberto Trotta, Licia Verde, Filippo Vernizzi, Adrian Vollmer, Yun Wang, Jochen Weller, and Tom Zlosnik. Cosmology and fundamental physics with the Euclid satellite. Living Reviews in Relativity, 21(1):2, April 2018. arXiv:1606.00180, doi:10.1007/s41114-017-0010-3.

[57] Neal Dalal, Olivier Dore, Dragan Huterer, and Alexander Shirokov. The imprints of primordial non-gaussianities on large-scale structure: scale dependent bias and abundance of virialized objects. Phys. Rev., D77:123514, 2008. arXiv:0710.4560, doi:10.1103/PhysRevD.77.123514.